Supplementary Information for

In-situ X-ray diffraction and radiography of iron–silicate–water–sulfur system simulating behaviors of light elements during early Earth's core–mantle segregation

Riko Iizuka-Oku*, Hirotada Gotou, Akio Suzuki, Hiroyuki Kagi

*Corresponding author (Riko Iizuka-Oku): riizuka@eqchem.s.u-tokyo.ac.jp

The PDF file contains:

Supplementary Figures S1-S6

Supplementary Tables S1-S2

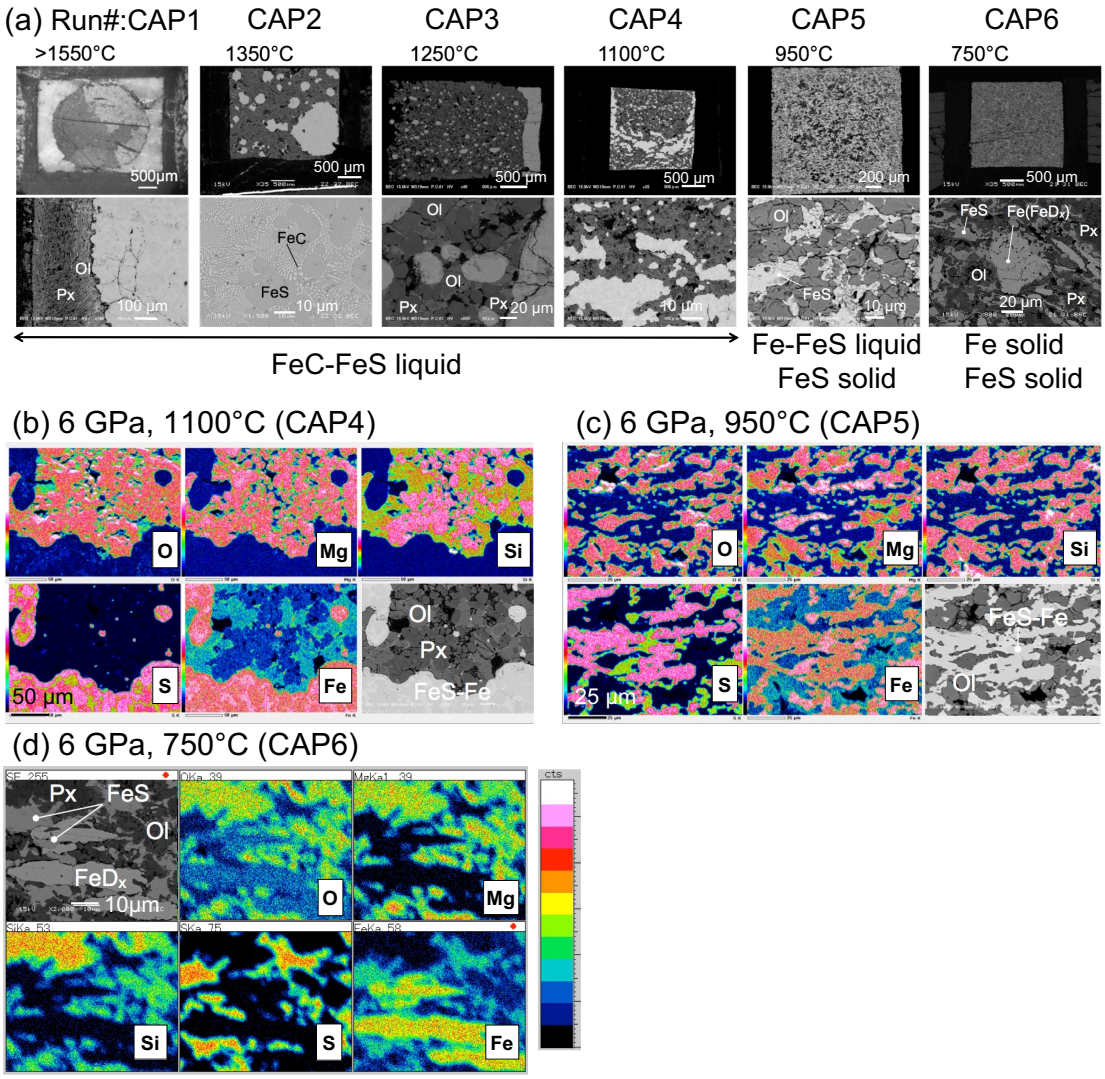

SFig. 1(a) Scanning electron microscope (SEM) images of samples recovered from quench experiments in order of higher-lower temperature (from left to right). The solid Fe phase was found in the sample quenched from lower temperature below 950°C in agreement with eutectic temperature of Fe–FeS system. (b–d) SEM images and elemental mappings of recovered samples containing sulfur quenched from **(b)** 1100°C, **(c)** 950°C, and **(d)** 750°C. Fe-C phase was identified from the micro-focused XRD measurements.

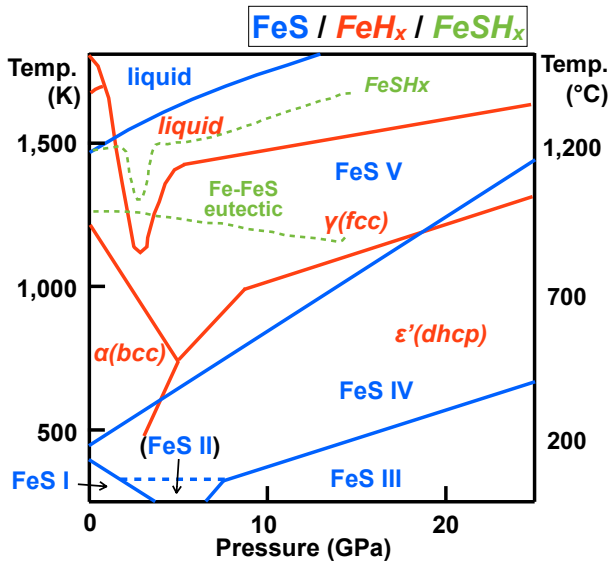

SFig. 2 Pressure–temperature phase diagrams of FeS, iron hydrides FeH_x, and $FeSH_x$ (x is hydrogen content). The phase boundaries of Fe and FeS are modified from [1–4]. The melting curve of $FeSH_x$ and eutectic of Fe–FeS are quoted from Shibazaki et al. [5] and references therein.

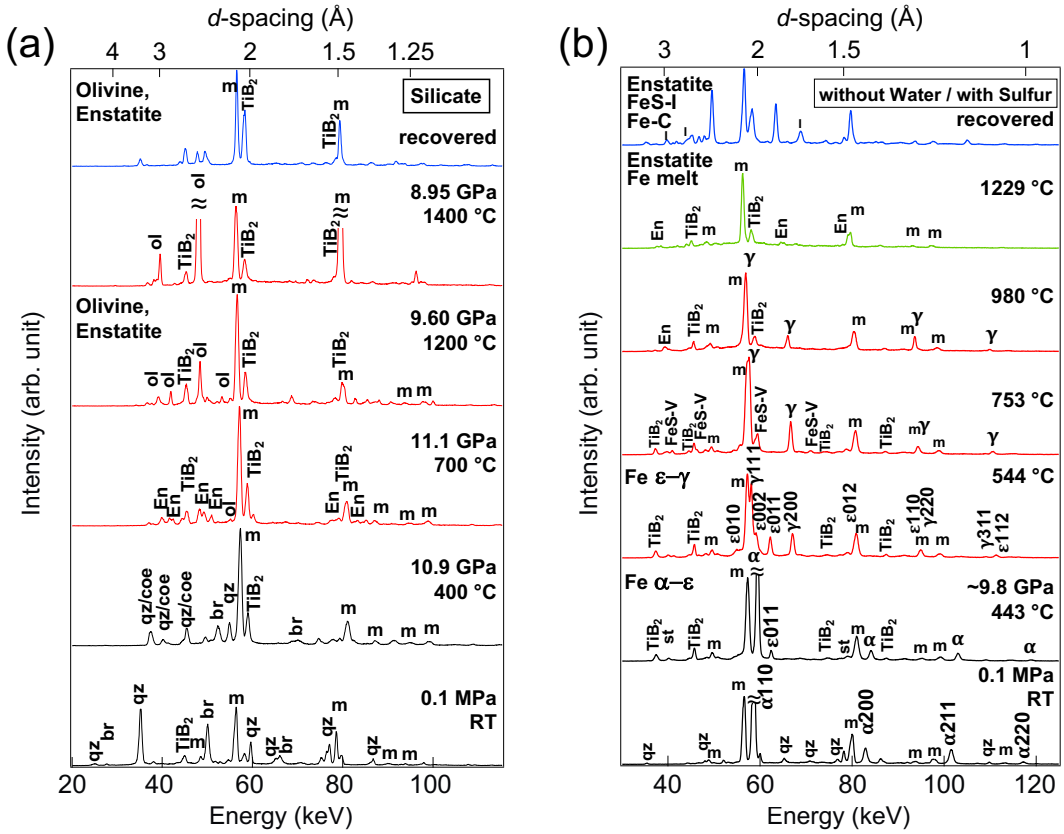

SFig. 3 Representative XRD patterns of samples **(a)** for silicate region with water and no sulfur (Run #1911-4) and **(b)** without water and with sulfur (Run #1806-3). Fe polymorphs are denoted as "α" for *bcc*-Fe, "ε" for *hcp*-Fe, and "γ" for *fcc*-Fe. "w" is FeO (wüstite). "V" and "I" are high-PT and ambient phases of FeS, respectively. For silicates, "en" is enstatite and "ol" is olivine. "br" is brucite. "qz", "coe" and "st" are, respectively, SiO_2 polymorphs, quartz, coesite and stishovite. "m" (MgO) is derived from a sleeve (thermal insulator) surrounding the sample capsule. TiB_2 is from the EBN heater.

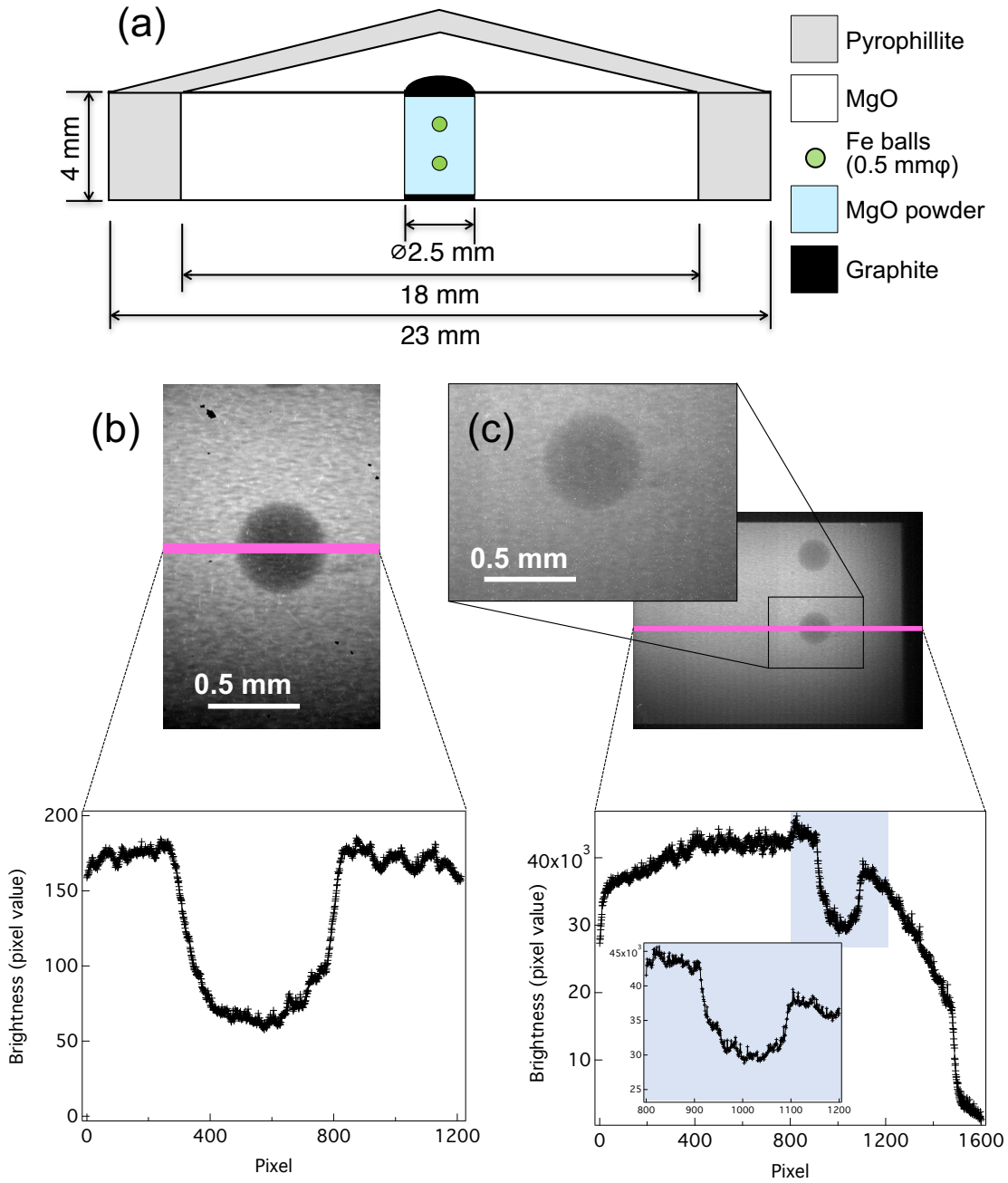

SFig. 4 (a) Cross-section of a dummy cell (a part of 6-8 MA type cell) containing two Fe balls of 0.5 mm diameter. **(b)** (upper) X-ray radiographic image of the lower Fe ball in **(a)** using the present imaging system and (lower) the resulting brightness profile along the horizontal pink area. The small black dots in the upper left corner come from dusts on the phosphorplate. **(c)** (middle) Full image (3.3 mm × 4.4 mm)

using the previous system by Nishida et al. [6] and (top) the magnified image with size corresponding to that obtained using the present system for comparison. (bottom) The brightness profile along the horizontal pink line in the middle image. Inset is a magnified profile of the shadow area. Original images were taken with a setting of maximum contrast. Curve fitting for calculating the boundary was not done because of the similar contrast between small Fe spheres and the surrounding materials.

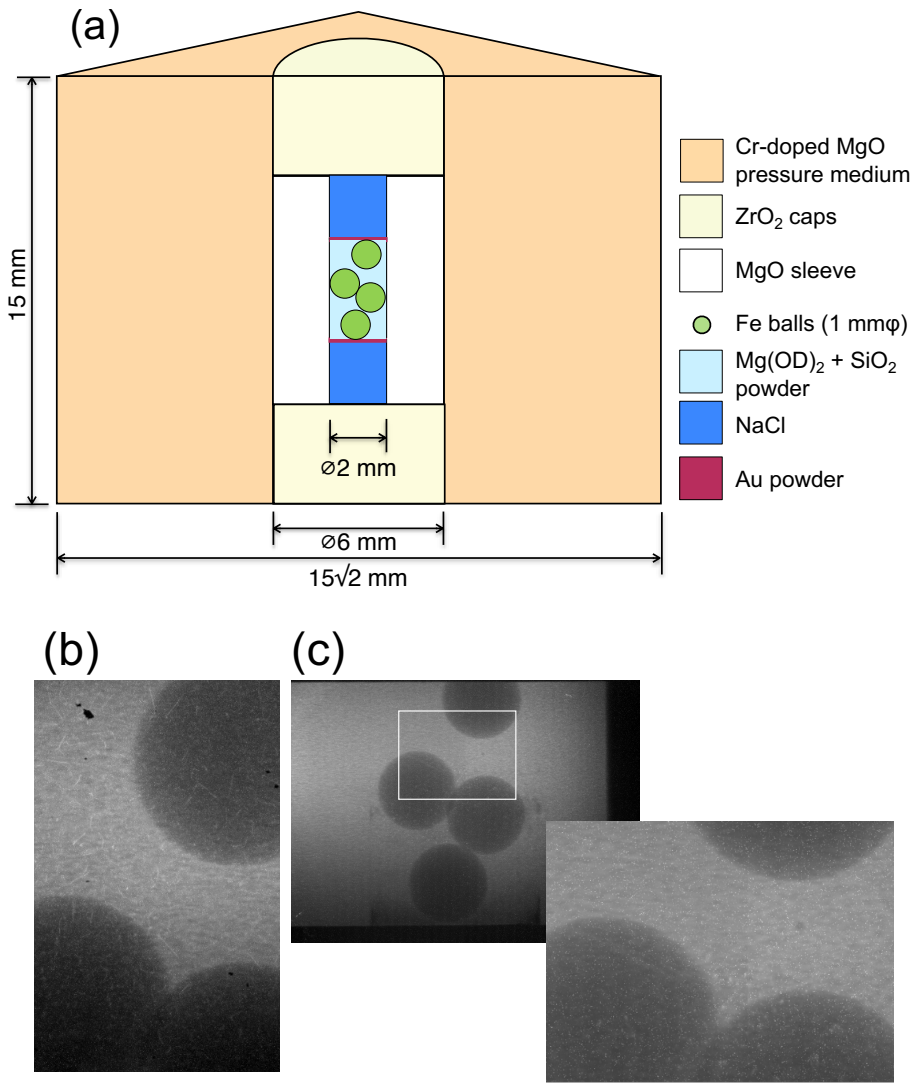

SFig. 5 (a) 6-6 MA type dummy cell containing four Fe balls of 1 mm diameter. **(b)** X-ray radiographic image of Fe balls in the lower center of the sample capsule acquired using the present imaging system. The image is 1 mm wide and 2 mm long. Small black dots in the upper left corner are caused by dust on the phosphor plate. **(c)** (upper left) Obtained X-ray radiographic image using the previous system [6] for comparison and (lower right) the magnified image with size corresponding to that obtained by the present system in **(b)**. Both original images were taken with a setting of maximum contrast.

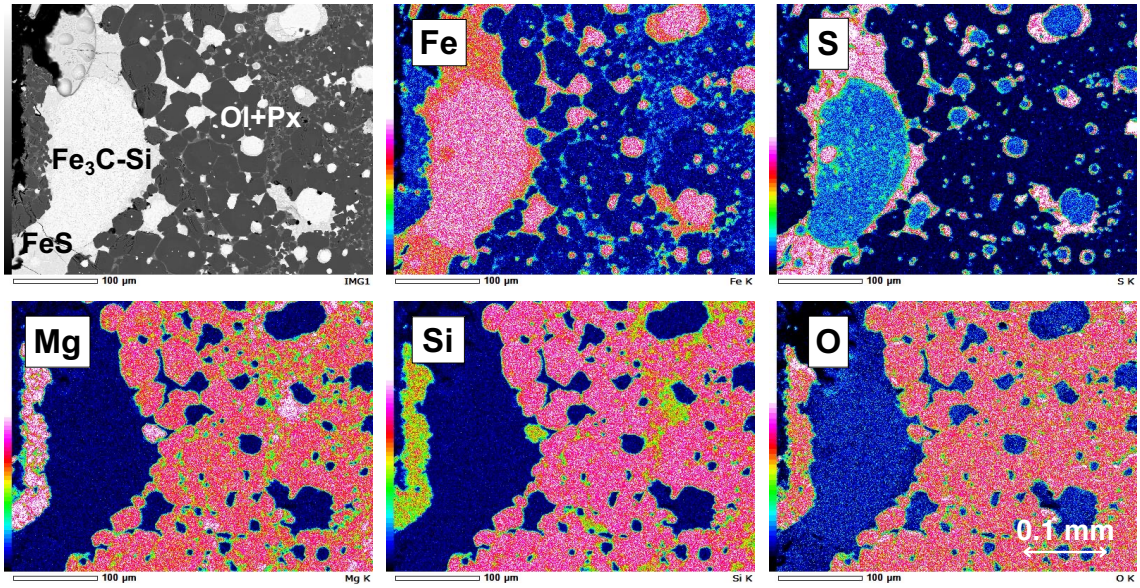

SFig. 6 Scanning electron microscope (SEM) image and elemental mappings of an anhydrous sample with sulfur recovered from 10 GPa, approx. 1600 °C (Run#1712-2). Fe_3C in both samples was identified from the micro-focused XRD measurements.

Supplementary Table S1 Experiment conditions and obtained products.

Run#	Sample	Water/S	P (GPa)	T (°C)	MaxT (°C)	XRD
		+/–: w/wo			XRD	Recovered sample
1906-1	Fe:$Mg(OD)_2$:SiO_2=2:1:1 mixture	+W-S	~10.3	1900*	1700	Fe_3C, Olivine(=Forsterite)
1911-4	Fe / $Mg(OD)_2$:SiO_2=1:1		~10.7	1400	1400	Fe_3C, Ol, Px
1906-2	Fe:$Mg(OD)_2$:SiO_2=2:1:1 + 5wt.%S	+W+S	~9.8	1900*	1200	Fe_3C, FeS-I, Ol, Px
1712-5			5~6	1734	1400	Fe_3C, FeS-I, Ol(=Fo), Px
1802-2			~4	1050	1050	Fe-bcc, FeS-I, Ol, Px (silicate not melt)
1806-1	Fe:FeS:$Mg(OD)_2$:SiO_2=2:2:1:1		5~6	1850	-	Fe_3C, FeS-I, Ol, Px
1806-3	Fe:MgO:SiO_2=2:1:1 + 5wt.%S	-W+S	~10	1600	1100	Fe_3C, FeS-I, Ol, En (silicate not melt)
1712-2			~4	1600	1600	Fe_3C, FeS-I, Ol, Px
1802-1			~4	1050	1050	Fe-bcc, FeS-I, Ol, Px (silicate not melt)

Note: ±W(S) represents samples with/without water (sulfur). FeS-I denotes ambient phase of iron sulfide (troilite). Px, pyroxene; Ol, olivine; Fo, forsterite. *Temperatures were estimated from the electrical power.

Supplementary Table S2 Summary of SEM results.

Exp.	Run#	Sample	Water/S	SEM analyses		n -data			SEM_Olivine	cation		Fe/(Mg+Fe)			n -data	SEM_Pyroxene	cation		Fe/(Mg+Fe)			n -data
			+/–: w/wo	Si content in Fe (wt%)	Si max		S content in silicate (wt.%)	S max	Mg^{2+}/Fe^{2+} ratio	Mg^{2+}	Fe^{2+}	average	max	min		Mg^{2+}/Fe^{2+} ratio	Mg^{2+}	Fe^{2+}	average	max	min	
In-situ	1906-1	Fe:Mg(OD)$_2$:SiO$_2$=2:1:1 mixture	+W-S	0.21(3)	0.70(4)	10	ND	ND	Mg1.96(1)Fe0.02(1)	1.94-1.98	0.02	0.01	0.02	0.02	13	ND	-	-	-	-	-	0
	1911-4	Fe / Mg(OD)$_2$:SiO$_2$=1:1		0.06(3)	0.14(3)	14	ND	ND	Mg1.5(4)Fe0.5(4)	0.81-1.86	1.16-0.12	0.26	0.59	0.06	17	Mg0.90(2)Fe0.09(2)	0.86-0.92	0.13-0.07	0.09	0.13	0.07	15
	1906-2	Fe:Mg(OD)$_2$:SiO$_2$=2:1:1 + 5wt.%S	+W+S	0.12(3)	0.19(3)	24	0.05	0.15	Mg1.5(1)Fe0.4(1)	1.28-1.62	0.64-0.32	0.23	0.33	0.16	11	Mg0.92(2)Fe0.08(2)	0.92	0.08	0.08	0.08	0.08	14
	1712-5			0.12	0.32	22	0.05	0.10	Mg1.93(3)Fe0.07(4)	1.85-1.96	0.18-0.05	0.04	0.09	0.02	11	ND	-	-	-	-	-	0
	1802-2			0.07	0.18	23	0.07	0.11	Mg1.01(9)Fe1.00(9)	0.87-1.28	1.16-0.73	0.50	0.57	0.36	24	Mg0.61(2)Fe0.38(2)	0.57-0.64	0.40-0.36	0.38	0.41	0.36	7
	1806-1	Fe:FeS:Mg(OD)$_2$:SiO$_2$=2:2:1:1		0.05(3)	0.08(3)	12	0.08(7)	0.16(5)	Mg1.4(2)Fe0.6(2)	0.88-1.57	1.11-0.36	0.31	0.56	0.21	12	Mg0.63(16)Fe0.36(12)	0.36-0.82	0.54-0.18	0.36	0.60	0.18	12
	1806-3	Fe:MgO:SiO$_2$=2:1:1 + 5wt.%S	-W+S	0.07(2)	0.13(3)	6	0.03(5)	0.10(5)	Mg1.62(2)Fe0.38(2)	1.59-1.65	0.40-0.36	0.19	0.20	0.18	6	Mg0.77(6)Fe0.24(6)	0.65-0.85	0.36-0.17	0.24	0.36	0.17	17
	1712-2			0.06	0.13	21	0.10	0.11	Mg1.3(2)Fe0.7(2)	0.99-1.69	0.98-0.45	0.35	0.50	0.21	10	Mg0.85(2)Fe0.14(2)	0.80-0.87	0.16-0.11	0.14	0.17	0.11	10
	1802-1			0.05	0.13	17	0.09	0.44	Mg1.31(16)Fe0.69(17)	1.14-1.57	0.87-0.43	0.35	0.43	0.22	8	Mg0.66(9)Fe0.34(9)	0.55-0.82	0.46-0.21	0.34	0.46	0.20	13
Quench	CAP1	Fe:FeS:Mg(OD)$_2$:SiO$_2$=2:2:1:1	+W+S	0.06	0.14	25	0.03	0.06	Mg1.3(3)Fe0.7(4)	0.78-1.73	1.22-0.31	0.34	0.61	0.15	16	Mg0.85(7)Fe0.17(6)	0.68-0.88	0.25-0.11	0.17	0.27	0.11	9
	CAP2			-	-	-	-	-	-	-	-	-	-	-	-	-	-	-	-	-	-	-
	CAP3			0.05	0.13	21	0.03	0.11	Mg1.1(3)Fe0.9(3)	0.54-1.43	1.43-0.58	0.43	0.73	0.29	11	Mg0.75(3)Fe0.26(3)	0.69-0.78	0.32-0.23	0.26	0.32	0.23	14
	CAP4			0.05(2)	0.12(2)	18	0.03	0.07	Mg1.19(16)Fe0.80(16)	0.78-1.35	1.2-0.64	0.40	0.61	0.32	14	Mg0.69(7)Fe0.32(7)	0.58-0.74	0.42-0.26	0.32	0.42	0.26	4
	CAP5			0.07	0.13	14	0.05	0.10	Mg1.10(11)Fe0.91(11)	0.93-1.22	1.07-0.79	0.45	0.54	0.39	8	ND	-	-	-	-	-	0
	CAP6			0.07(0)	0.14(1)	12	0.07(7)	0.18(6)	Mg1.1(2)Fe0.9(2)	0.78-1.41	1.21-0.65	0.46	0.61	0.32	8	Mg0.67(4)Fe0.33(4)	0.63-0.7	0.38-0.30	0.35	0.38	0.30	5

Note: ±W(S) represents samples with/without water (sulfur); n-data, number of data points; ND, not detected. Numbers in parentheses for Mg^{2+}/Fe^{2+} ratio of silicates are errors in the last digits and calculated from standard deviation. CAP2 was not analyzed by SEM.

References

[1] Antonov VE, Baier M, Dorner B, et al. High-pressure hydrides of iron and its alloys. J Phys Condens Matter 2002;14:6427–6445.

[2] Fukai Y, Mori K, Shinomiya H. The phase diagram and superabundant vacancy formation in Fe-H alloys under high hydrogen pressures. J Alloys Compd. 2003;348:105–109.

[3] Klotz S, Le Godec Y, Strässle T, et al. The α-γ-ε triple point of iron investigated by high pressure-high temperature neutron scattering. Appl Phys Lett. 2008;93:091904.

[4] Urakawa S, Someya K, Terasaki H, et al. Phase relationships and equations of state for FeS at high pressures and temperatures and implications for the internal structure of Mars. Phys Earth Planet Inter. 2004;143–144:469–479.

[5] Shibazaki Y, Ohtani E, Terasaki H, et al. Effect of hydrogen on the melting temperature of FeS at high pressure: Implications for the core of Ganymede. Earth Planet Sci Lett. 2011;301:153–158.

[6] Nishida K., Suzuki A., Terasaki H. et al. Towards a consensus on the pressure and composition dependence of sound velocity in the liquid Fe–S system. Phys Earth Planet Inter. 2016;257:230–239.